

Control of Microtubule Dynamics by Stu2p Is Essential for Spindle Orientation and Metaphase Chromosome Alignment in Yeast

Karena A. Kosco,* Chad G. Pearson,[†] Paul S. Maddox,[†] Peijing Jeremy Wang,^{*‡} Ian R. Adams,^{§||} E. D. Salmon,[†] Kerry Bloom,[†] and Tim C. Huffaker^{*¶}

*Department of Molecular Biology and Genetics, Cornell University, Ithaca, New York 14853-2703;

[†]Department of Biology, University of North Carolina–Chapel Hill, Chapel Hill, North Carolina 27599-3280; and [§]MRC Laboratory of Molecular Biology, Cambridge CB2 2QH, United Kingdom

Submitted May 15, 2001; Revised July 3, 2001; Accepted July 5, 2001

Monitoring Editor: Tim Stearns

Stu2p is a member of a conserved family of microtubule-binding proteins and an essential protein in yeast. Here, we report the first *in vivo* analysis of microtubule dynamics in cells lacking a member of this protein family. For these studies, we have used a conditional Stu2p depletion strain expressing α -tubulin fused to green fluorescent protein. Depletion of Stu2p leads to fewer and less dynamic cytoplasmic microtubules in both G1 and preanaphase cells. The reduction in cytoplasmic microtubule dynamics is due primarily to decreases in both the catastrophe and rescue frequencies and an increase in the fraction of time microtubules spend pausing. These changes have significant consequences for the cell because they impede the ability of cytoplasmic microtubules to orient the spindle. In addition, recovery of fluorescence after photobleaching indicates that kinetochore microtubules are no longer dynamic in the absence of Stu2p. This deficiency is correlated with a failure to properly align chromosomes at metaphase. Overall, we provide evidence that Stu2p promotes the dynamics of microtubule plus-ends *in vivo* and that these dynamics are critical for microtubule interactions with kinetochores and cortical sites in the cytoplasm.

INTRODUCTION

The dynamic nature of the microtubule cytoskeleton is essential for its function in a variety of cellular processes such as organelle organization and chromosome segregation. Interestingly, microtubules *in vivo* are much more dynamic than microtubules assembled from pure tubulin. To account for the dynamics of microtubules in cells, much effort has been directed toward the identification and characterization of proteins that regulate microtubule dynamics (Desai and Mitchison, 1997; Cassimeris, 1999). Although an increasing number of proteins that influence microtubule dynamics in

vitro have been identified, their relative importance and precise roles *in vivo* are not yet well understood.

Individual microtubules exhibit stochastic transitions between states of growth and shrinkage, a behavior known as dynamic instability (Desai and Mitchison, 1997). Transitions from growth to shrinkage are called catastrophes; transitions from shrinkage to growth are rescues. Thus, microtubule behavior can be defined by four parameters: the growth rate, the shrinkage rate, the catastrophe frequency, and the rescue frequency. Additionally, microtubules sometimes enter a paused state, in which they neither grow nor shrink. Proteins that regulate microtubule dynamics have been classified as either microtubule-stabilizing or microtubule-destabilizing factors on the basis of their net effect on microtubule polymerization. Maintaining the proper balance among these regulatory factors must be critical for controlling the dynamics of microtubules in the cell.

Previously, we described the identification of Stu2p, an essential microtubule-binding protein in yeast (Wang and Huffaker, 1997). Stu2p is a member of the protein family that includes *Schizosaccharomyces pombe* Dis1 (Nabeshima *et al.*, 1995), human TOGp (Charrasse *et al.*, 1998), *Caenorhabditis*

Present addresses: [‡]Whitehead Institute for Biomedical Research, Cambridge, MA 02142-1479; ^{||}Wellcome/CRC Institute of Cancer and Developmental Biology, Cambridge University, Cambridge CB2 1QR, United Kingdom.

[¶] Corresponding author. E-mail address: tch4@cornell.edu.

Abbreviations used: DAPI, 4',6-diamidino-2-phenylindole; FRAP, fluorescence redistribution after photobleaching; GFP, green fluorescent protein; SPB, spindle pole body.

Table 1. Yeast strains

Strain	Genotype	Source
CUY25	<i>MATa leu2-3,112 his3-Δ200 ura3-52 ade2</i>	This study
CUY546	<i>MATa/MATα leu2-3,112/leu2-3,112 his3-Δ200/his3-Δ200 ura3-52/ura3-52 ade2/ADE2</i>	This study
CUY1046	<i>MATa/MATα stu2-Δ1::HIS3/STU2 leu2-3,112/leu2-3,112 his3-Δ200/his3-Δ200 ura3-52/ura3-52 ade2/ADE2</i>	This study
CUY1070	<i>MATa stu2-10::LEU2 leu2-3,112 his3-Δ200 ura3-52</i>	This study
CUY1087	<i>MATa stu2-Δ1::HIS3 leu2-3,112 his3-Δ200 ura3-52 (pWP98: P_{GAL1}-STU2 URA3 CEN6 ARSH4)</i>	This study
CUY1088	<i>MATa stu2-10::URA3 leu2-3,112 his3-Δ200 ura3-52</i>	This study
CUY1089	<i>MATα stu2-10::URA3 leu2-3,112 his3-Δ200 ura3-52 ade2-101</i>	This study
CUY1090	<i>MATa his3-Δ200 leu2-3,112 ura3-52</i>	This study
CUY1097	<i>MATa/MATα stu2-10::URA3/stu2-10::URA3 leu2-3,112/leu2-3,112 his3-Δ200/his3-Δ200 ura3-52/ura3-52 ADE2/ade2</i>	This study
CUY1142	<i>MATα stu2-13::URA3 leu2 his3-Δ200 ura3-52 lys2-801</i>	This study
CUY1143	<i>MATa stu2-13::URA3 leu2 his3-Δ200 ura3-52 ade2-101</i>	This study
CUY1147	<i>MATa ura3-52 trp1-Δ1 ade2-101 lys2-801 P_{ACE1}-UBR1 P_{ACE1}-ROX1 stu2Δ::URA3::P_{ANB1}-UB-R-STU2</i>	This study
CUY1148	<i>MATa ura3-52 trp1-Δ1 ade2-101 lys2-801 P_{ACE1}-UBR1 P_{ACE1}-ROX1 ura3-52::URA3</i>	This study
CUY1149	<i>MATa mad2Δ::URA3 leu2-3,112 ura3-52 his3-Δ200 ade2</i>	This study
CUY1151	<i>MATa stu2-10::LEU2 mad2Δ::URA3 leu2-3,112 ura3-52 his3-Δ200</i>	This study
CUY1243	<i>MATa ura3-52 trp1-Δ1 ade2-101 lys2-801 P_{ACE1}-UBR1 P_{ACE1}-ROX1 stu2Δ::URA3::P_{ANB1}-UB-R-STU2 TUB1::TRP1::GFP-TUB1</i>	This study
CUY1244	<i>MATa ura3-52 trp1-Δ1 ade2-101 lys2-801 P_{ACE1}-UBR1 P_{ACE1}-ROX1 ura3-52::URA3 TUB1::TRP1::GFP-TUB1</i>	This study
CUY1247	<i>MATα leu2-3,112 ura3-52 his3-Δ200 STU2-GFP::HIS5</i>	This study
CUY1257	<i>MATα stu2-10::URA3 leu2 ura3-52 his3-Δ200 trp1-Δ1 ade2</i>	This study
CUY1258	<i>MATα stu2-10::LEU2 leu2 ura3-52 his3-Δ200 trp1-Δ1 lys2-801</i>	This study
CUY1259	<i>MATa stu2-10::LEU2 leu2 ura3-52 his3-Δ200 trp1-Δ1</i>	This study
CUY1260	<i>MATa stu2-13::URA3 leu2 ura3-52 his3-Δ200 trp1-Δ1 lys2-801</i>	This study
KBY2660.1	<i>MATa ura3-52 trp1-Δ1 ade2-101 lys2-801 P_{ACE1}-UBR1 P_{ACE1}-ROX1 stu2Δ::URA3::P_{ANB1}-UB-R-STU2 cse4Δ::HPH (pKK1: Cse4-GFP TRP1)</i>	This study
KBY9	<i>MATa dhc1::HIS3 leu2 ura3 his3 ade1 met14</i>	K. Bloom
DS615	<i>MATα kip3-Δ1::HIS3 leu2-3,112 ura3-52 his3-Δ200 trp1-Δ1</i>	D. Roof
MAY2058	<i>MATα cin8Δ::LEU2 leu2-3,112 ura3-52 his3-Δ200 lys2-801</i>	M.A. Hoyt
MAY2059	<i>MATa cin8Δ::LEU2 leu2-3,112 ura3-52 his3-Δ200 ade2-101</i>	M.A. Hoyt
MAY2079	<i>MATα kip1::HIS3 leu2-3,112 ura3-52 his3-Δ200 lys2-801</i>	M.A. Hoyt
MS524	<i>MATa kar3-101::LEU2 leu2-3,112 ura3-52 ade2-101</i>	M. Rose
MS2354	<i>MATα kip2-Δ::TRP1 leu2-3,112 ura3 trp1-Δ1</i>	M. Rose
MS4306	<i>MATa kar9-Δ2::HIS3 leu2-3,112 ura3-52 his3-Δ200 ade2-101</i>	M. Rose
ZMY60	<i>MATa ura3-52 trp1-Δ1 ade2-101 lys2-801 P_{ACE1}-UBR1 P_{ACE1}-ROX1</i>	K. Struhl

elegans ZYG-9 (Matthews *et al.*, 1998), *Drosophila* Msp (Cullen *et al.*, 1999), and *Xenopus* XMAP215 (Tournebize *et al.*, 2000). All of these proteins localize to the microtubule-organizing center and spindle during mitosis. *dis1*, *zyg-9*, and *msps* mutations cause improper spindle formation and chromosome missegregation.

XMAP215 has been shown to have a direct effect on microtubule dynamics. XMAP215 promotes the polymerization of pure tubulin in vitro by increasing the growth rate without reducing catastrophes or stimulating rescues (Vasquez *et al.*, 1994). However, in *Xenopus* egg extracts, the primary function of XMAP215 is to suppress catastrophes. As XMAP215 has no intrinsic ability to suppress catastrophes, it has been proposed that the role in XMAP215 in extracts is to compete for access to microtubules with the microtubule-destabilizing protein XKCM1 (Tournebize *et al.*, 2000). These results highlight the commonly held belief that microtubule dynamics in cells are likely to be determined by the complex interplay of regulatory factors. Unfortunately, such complex regulation of microtubule dynamics has been difficult to study in intact cells.

In this study we present the first in vivo analysis of microtubule dynamics in cells lacking a member of this protein family. With the use of *stu2* mutant yeast cells expressing tubulin fused to green fluorescent protein (GFP; Carminati and Stearns, 1997; Shaw *et al.*, 1997b; Tirnauer *et al.*, 1999; Adames and Cooper, 2000), we show that Stu2p promotes the dynamics of cytoplasmic and spindle microtubules in *Saccharomyces cerevisiae*, contrary to the role of XMAP215 in *Xenopus* extracts. In addition, we show that the promotion of microtubule dynamics by Stu2p is required for proper spindle orientation and metaphase chromosome alignment.

MATERIALS AND METHODS

Yeast Strains, Media, and Plasmids

The yeast strains used are listed in Table 1. YPD and SD media were prepared as described (Sherman, 1991). To deplete Stu2p in *stu2^{eu}* strains, cupric sulfate (CuSO₄) was added to SD media to a final concentration of 500 μM. Cells were treated with 3 μg/ml α-factor or 100 mM hydroxyurea for 2 h to arrest them in G1 or S phase, respectively.

The plasmid encoding GFP-Tub1p under control of the *TUB1* promoter, pAFS125 (Straight *et al.*, 1997), was a gift from Dr. Andrew Murray (Harvard University, Cambridge, MA). The *KpnI* to *NotI* fragment of pAFS125 containing *GFP-TUB1* was ligated into *KpnI*- and *NotI*-digested pRS404 to create pKAK101. pKAK101 was linearized with *NsiI* and transformed into CUY1147 and CUY1148 to create CUY1243 and CUY1244, respectively. The plasmid encoding Cse4-GFP, pKK1 (Chen *et al.*, 2000), was a gift from Dr. Richard Baker (University of Massachusetts Medical School, Worcester).

GFP Tagging of *Stu2p*

pYGFP, a gift from Brendan Cormack (Johns Hopkins School of Medicine, Baltimore), contains a version of GFP with codons optimized for usage in yeast (Cormack *et al.*, 1997). The *HIS5* gene from *S. pombe* was cloned into the *BamHI* and *EcoRI* sites of pYGFP to create pHY181. The *yGFP::HIS5* sequence was amplified from pHY181 by PCR with the use of the forward primer 5'-GAATTG-AAAAAATGAAGCCAAATCAAGACGGGAAGGGACAACCA-GGACGATGTCTAAAGGTGAAGAAT-3' and the reverse primer 5'-TCAAGTTGAAGACTATATATTTATTGAGTTTATGTTATGGG-GAGGCTACCTGGATGGCGGCGTTAGTAT. The resulting DNA fragment contained 50 bp of sequence immediately upstream of the *STU2* stop codon followed by *yGFP*, *HIS5*, and then 50 bp of *STU2* sequence beginning 3 bp downstream of the stop codon. This fragment was transformed into the diploid yeast strain CUY546 to fuse GFP to the C-terminal end of the chromosomal *STU2* gene. One His⁺ transformant was sporulated and dissected to generate CUY1247.

Stu2p Depletion Strain

We created a yeast strain in which, upon addition of copper, there is a simultaneous repression of *STU2* mRNA synthesis and degradation of *Stu2p* (Moqtaderi *et al.*, 1996). Briefly, a 404-bp fragment of the *STU2* gene (beginning with ATG) was subcloned into the *SpeI* site of the ZM168 polylinker producing pKAK59. pKAK59 was digested with *KpnI* and *XbaI*, and the resulting *P_{ANB1}-Ub-R-STU2* fragment was ligated into the same sites of pRS406 (Sikorski and Hieter, 1989). The resulting plasmid, pKAK60 was linearized with *HindIII*, transformed into ZMY60, and plated onto selective media. Integrating linearized pRS406 into ZMY60 created the control strain (CUY1148). The Ura⁺ transformants were then tested for copper sensitivity by comparing their growth with CUY1148 on SD plates containing CuSO₄ at 250 or 500 μM. One Ura⁺ transformant was selected (CUY1147) that was inviable on SD plates containing 500 μM CuSO₄, a concentration that allowed growth of CUY1148.

stu2 Temperature-Sensitive Mutants

STU2 was amplified by PCR with primers 5'-GGGACCAAATAG-CATTAC-3' and 5'-GTGCAGTGTGCTTATCTC-3' under mutagenic conditions with the use of 7 mM MgCl₂ (Muhlrad *et al.*, 1992). PCR products were digested with *BamHI* and *SphI* and ligated into the larger *BamHI-SphI* fragment of pS2 (*stu2-1 LEU2 CEN6 ARSH4*; Wang and Huffaker, 1997). To screen for conditional-lethal mutants, the library was transformed into the haploid strain CUY1087 whose viability is dependent on the expression of the plasmid-borne *STU2* from the *GAL1* promoter. Leu⁺ transformants were screened for conditional lethality on YPD plates at various temperatures.

Stu2p Antibody and Western Blots

The 1.16-kb *KpnI* fragment from pWP82 (Wang and Huffaker, 1997) was cloned into the *KpnI* site of pQE-31 (QIAGEN Inc., Chatsworth, CA) to make pWP86; this construct encodes a polypeptide containing the 385 carboxy-terminal amino acids of *Stu2p* fused to the His₆ tag. The 44-kDa fusion protein was expressed in *Escherichia coli* strain M15 and purified on Ni²⁺-NTA resin under denaturing conditions. Rabbit antiserum to this polypeptide was produced by

the Center for Research Animal Resources at Cornell University (Ithaca, NY).

Total yeast extracts were made by grinding cells that had been rapidly frozen in liquid nitrogen (Sorger *et al.*, 1994). Forty micrograms of total protein was resolved by SDS-PAGE and then transferred to nitrocellulose. The rabbit polyclonal anti-*Stu2p* antibody was used at a 1:5000 dilution. The secondary antibody, HRP-conjugated donkey anti-rabbit (Amersham Pharmacia Biotechnology, Piscataway, NJ) was used at a 1:10,000 dilution and was visualized with the use of an enhanced chemiluminescence system (Amersham Pharmacia Biotechnology).

Fluorescence Microscopy and Image Analysis

Indirect immunofluorescence was performed as described previously (Pasqualone and Huffaker, 1994). Rat monoclonal anti-yeast α -tubulin antibody, YOL1/34 (Kilmartin *et al.*, 1982), was provided by J. Kilmartin (Medical Research Council, Cambridge, United Kingdom). Fluorescein goat anti-rat secondary antibody was purchased from Cappel Research Products (Durham, NC). 4',6-diamidino-2-phenylindole (DAPI) staining of DNA was done as described previously (Sullivan and Huffaker, 1992). Laser photobleaching of GFP-Tub1p in live cells and statistical analysis of FRAP was performed as described previously (Maddox *et al.*, 2000).

Time-lapse analysis of live cells was performed on cells grown at 23°C in SD media supplemented with adenine, lysine, and CuSO₄. Slides were prepared and images captured as described by Shaw *et al.* (1997a). Time lapse series were acquired at 10 or 20 s intervals. The 2 × 2 binned images were acquired in Z-series either five planes 0.75 μm apart or six planes 0.5 μm apart. At each time point, we measured the length of the microtubule in the *x-y* plane (A); its height in the *z*-axis (B) was determined by counting the number of planes containing an in-focus portion of the microtubule. The total length of the microtubule at each time point was then calculated to be C, where $A^2 + B^2 = C^2$.

Linear regression analysis was used to obtain rates of microtubule growth and shrinkage. Growth and shrinkage events were defined by a line with an R^2 value of ≥ 0.85 and a net change in length of ≥ 0.5 μm. Pauses were defined as events that lasted ≥ 30 s in which no significant growth or shrinkage occurred. Catastrophes were defined as transitions to shrinkage after a growth or pause; rescues were defined as transitions to growth after a shrinkage or pause. The frequencies of catastrophe and rescue were calculated by dividing the total number of events by the total time that all microtubules spent pausing and growing or pausing and shrinking, respectively.

Variations around mean values are given as SDs. Comparisons of statistical significance were by unpaired *t* test.

RESULTS

Depletion of *Stu2p* Causes a Mitotic Arrest

An *stu2* conditional depletion strain was constructed based on the methods first described by Moqtaderi *et al.* (Moqtaderi *et al.*, 1996). Addition of copper ions to the medium causes simultaneous repression of *STU2* mRNA synthesis and degradation of *Stu2p*; hence, we refer to this strain as *stu2^{cu}*. In this strain, *ROX1* and *UBR1* are under control of a tightly regulated copper-inducible promoter. *UBR1* encodes the N-end recognition component of the ubiquitin degradation pathway. *Rox1p* is a transcriptional repressor of the *ANB1* gene. The *STU2* gene is replaced by a derivative that contains an N-end rule recognition signal for rapid ubiquitin-dependent degradation and is driven by the *ANB1* promoter. In the absence of copper, neither the repressor nor the protein degradation system is active, and *Stu2p* is expressed. Addition of copper sulfate activates both systems

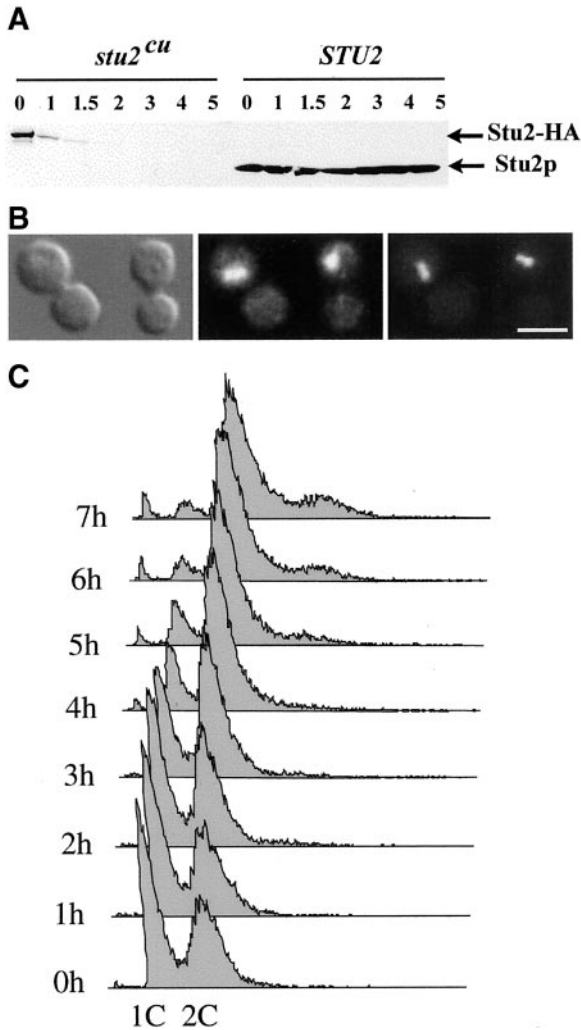


Figure 1. Phenotype of Stu2p-depleted cells. (A) Time course of Stu2p depletion. *STU2* (CUY1148) and *stu2^{cu}* (CUY1147) cells were diluted into copper-containing media for the time (h) indicated above each lane. Equal amounts of protein extract were subjected to SDS-PAGE followed by immunoblotting with the use of anti-Stu2p antibody. Note that in the construction of the *stu2^{cu}* strain, an HA epitope tag is fused to the N-terminus of Stu2p. (B) *stu2^{cu}* (CUY1147) cells after 4 h copper-containing medium. Left, DIC; middle, DAPI staining of DNA; right, immunofluorescence with the use of Tub2p antibody. Bar, 4 μ m. (C) DNA content of *stu2^{cu}* cells. CUY1243 cells were grown asynchronously at 23°C and shifted into copper-containing medium for the times indicated. The DNA content of individual cells was determined by flow cytometry (Haase and Lew, 1997).

and causes a decrease in Stu2p levels. Stu2p is undetectable in *stu2^{cu}* cells by 2 h after addition of copper (Figure 1A). Cells lacking Stu2p arrest in mitosis. After 6 h of growth at 23°C in copper-containing medium, most of the cells were large budded (74%) and contained replicated but unsegregated chromosomes (Figure 1, B and C). Immunofluorescence microscopy with the use of anti- α -tubulin antibody showed that most of these cells (>80%) possessed preanaphase spindles (Figure 1B).

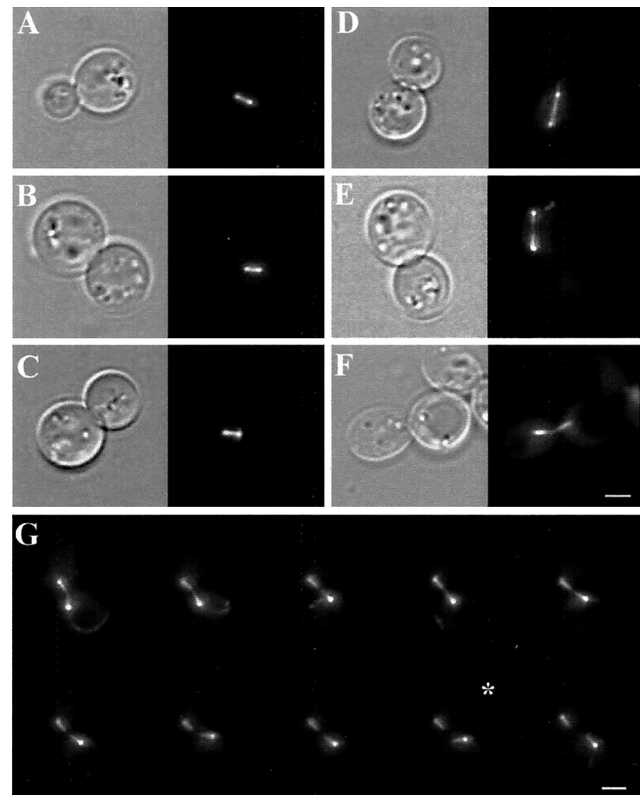


Figure 2. Analysis of spindles in *stu2^{cu}* cells expressing GFP-Tub1p. (A–F) DIC (left) and GFP-Tub1p fluorescence of microtubules (right) in *STU2* (CUY1244) and *stu2^{cu}* cells (CUY1243). (A) Preanaphase spindle in *STU2* cell; (B and C) similar short spindles in *stu2^{cu}* cells. (D) Elongated \sim 3- μ m spindle in *STU2* cell; (E and F) \sim 3- μ m spindles in *stu2^{cu}* cells. (G) Time-lapse images taken at 1-min intervals of a *stu2^{cu}* cell showing a spindle breaking down before reaching full length. Spindle breakage occurs in the panel labeled with the asterisk. Bars, 2 μ m.

We analyzed spindles in live *STU2* and *stu2^{cu}* cells expressing GFP-Tub1p that were grown in copper-containing medium for at least 4 h (Figure 2). The average length of the preanaphase spindles in *STU2* cells (Figure 2A) was $1.25 \pm 0.28 \mu$ m ($n = 43$). The average length of preanaphase spindles in large-budded *stu2^{cu}* cells (Figure 2, B and C) was $1.08 \pm 0.28 \mu$ m ($n = 52$), a small but statistically significant difference in spindle length ($p = 0.004$ by unpaired t test). In addition, 15% of *stu2^{cu}* large-budded cells contained partially elongated spindles up to 5.0 μ m in length. However, none possessed fully elongated anaphase spindles, typically 8–10 μ m in length in *STU2* cells. In contrast to the GFP fluorescence of *STU2* spindles (Figure 2D), which is relatively uniform along their lengths, the fluorescence of 3–5 μ m spindles in *stu2^{cu}* cells was brightest at the poles and gradually diminished away from the poles (Figure 2, E and F). These *stu2^{cu}* spindles would occasionally bend and eventually break despite failing to elongate more than half the length of a normal anaphase spindle (Figure 2G).

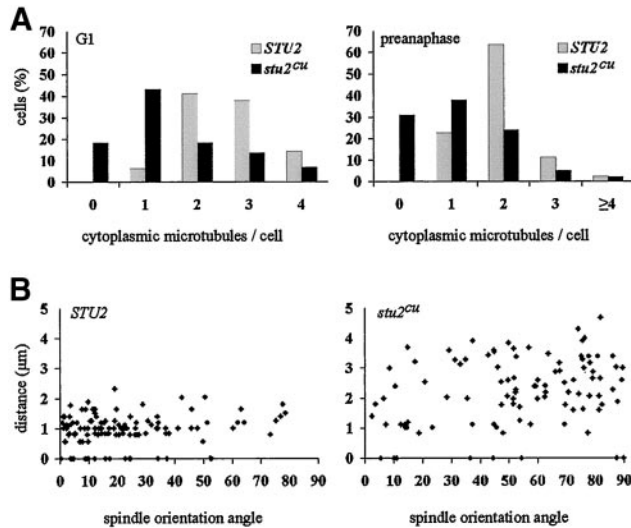


Figure 3. Cytoplasmic microtubule number and spindle orientation. (A) Asynchronous *STU2* (CUY1244) and *stu2^{cu}* (CUY1243) cells were shifted into copper-containing media for 4 h. Cytoplasmic microtubules were visualized by GFP-Tub1p fluorescence. (B) Asynchronous *stu2^{cu}* (CUY1243) cells and hydroxyurea-arrested *STU2* (CUY1244) cells were shifted into copper-containing media for 4 h. GFP-Tub1p was visualized in live cells, and images were collected of budded cells containing short spindles. The spindle angle was calculated as the angle between a straight line drawn through the mother-bud neck axis and a second line drawn through the spindle. Spindle distance is the distance between the bud-proximal end of the spindle and the bud neck.

Cells Lacking *Stu2p* Contain Fewer Cytoplasmic Microtubules

We counted the number of cytoplasmic microtubules in live *STU2* and *stu2^{cu}* cells expressing GFP-Tub1p that were grown in copper-containing medium for at least 4 h. *stu2^{cu}* cells contained on average just over half the number of cytoplasmic microtubules as *STU2* cells (Figure 3A). In unbudded G1 cells that contain a single SPB, *STU2* and *stu2^{cu}* cells had an average of 2.6 ± 0.8 and 1.5 ± 1.2 cytoplasmic microtubules per cell, respectively ($n = 63, 44$; $p < 0.001$). In cells that contained preanaphase spindles and two SPBs, the *STU2* and *stu2^{cu}* cells had an average of 1.9 ± 0.7 and 1.1 ± 1.0 microtubules per cell, respectively ($n = 44, 55$; $p < 0.001$). Significantly, 18% of unbudded *stu2^{cu}* cells and 31% of *stu2^{cu}* cells with preanaphase spindles contained no cytoplasmic microtubules. In contrast, every *STU2* cell we examined contained at least one cytoplasmic microtubule.

We did not find a statistically significant difference between cytoplasmic microtubule lengths in *STU2* and *stu2^{cu}* cells. The average length of cytoplasmic microtubules in unbudded cells was $1.3 \pm 0.6 \mu\text{m}$ for *STU2* cells and $1.4 \pm 0.8 \mu\text{m}$ for *stu2^{cu}* cells ($n = 73, 61$). For cells that contained spindles, the average cytoplasmic microtubule length was $1.3 \pm 0.7 \mu\text{m}$ for *STU2* cells and $1.4 \pm 1.1 \mu\text{m}$ for *stu2^{cu}* cells ($n = 62, 61$).

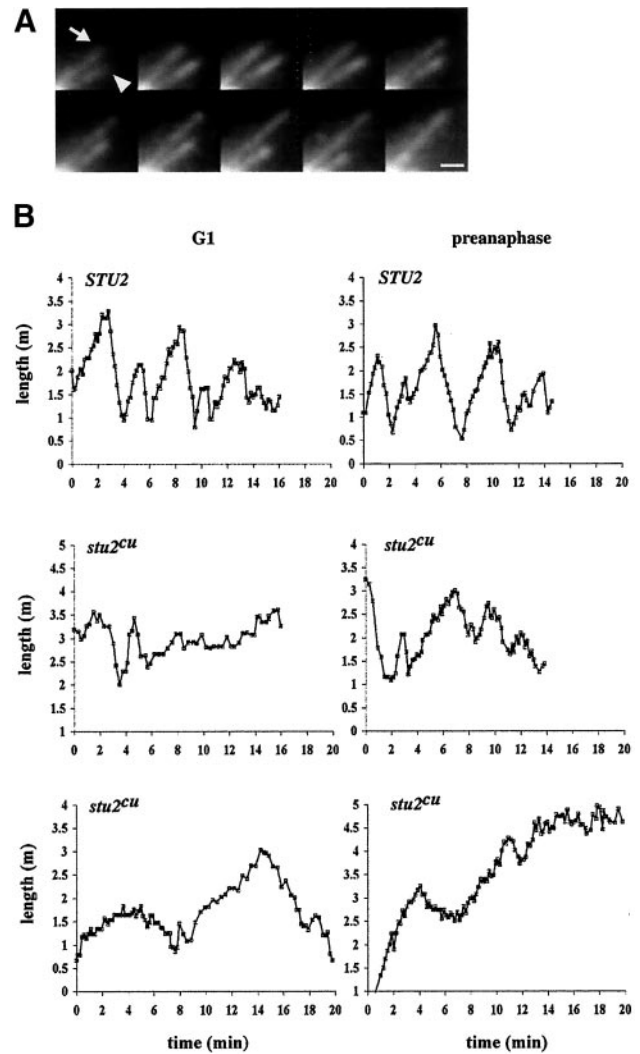


Figure 4. Cytoplasmic microtubule dynamics in *STU2* (CUY1244) and *stu2^{cu}* (CUY1243) cells expressing GFP-Tub1p. (A) Cytoplasmic microtubules in a single *STU2* G1 cell. Images show two-dimensional projections of Z-focal plane series at 20-s intervals. One microtubule (arrow) grew throughout this time course. A second (arrowhead) grew and then shrank back to the SPB. The SPB is located in the lower left corner. Bar, $1 \mu\text{m}$. (B) Plots were constructed from measurements of cytoplasmic microtubule length (see MATERIALS AND METHODS) versus time for G1 (left panels) and preanaphase (right panels) cells.

Cytoplasmic Microtubules Are Less Dynamic in *Stu2p*-depleted Cells

Cytoplasmic microtubule dynamics were measured in live *STU2* and *stu2^{cu}* cells expressing GFP-Tub1p after growth on copper-containing medium for at least 3 h (Figure 4A). We analyzed both G1 cells that lacked spindles and preanaphase cells that contained short bipolar spindles. Because the *stu2^{cu}* population lacked cells with long anaphase spindles, we did not analyze anaphase cells in the *STU2* population. Representative microtubule life history plots are shown in Figure 4B, and the data described in this section are listed in Table 2.

Table 2. Cytoplasmic microtubule dynamics

	G1		Preanaphase	
	<i>STU2</i>	<i>stu2^{cu}</i>	<i>STU2</i>	<i>stu2^{cu}</i>
Rates ($\mu\text{m}/\text{min}$)				
Growing	0.79 ± 0.38 (17)	0.63 ± 0.45 (21)	0.86 ± 0.37 (22)	1.00 ± 0.48 (19)
Shrinking	1.55 ± 1.08 (20)	0.85 ± 0.57 (24)	1.36 ± 0.58 (26)	1.28 ± 0.51 (23)
Frequencies (event/s)				
Catastrophe	0.0071 (20)	0.0035 (22)	0.0085 (20)	0.0054 (21)
Rescue	0.0063 (13)	0.0030 (18)	0.0092 (18)	0.0038 (14)
Event durations (min)				
Growing	1.99 ± 1.56 (17)	2.40 ± 1.83 (21)	1.44 ± 0.87 (22)	1.49 ± 1.13 (19)
Shrinking	1.05 ± 0.72 (20)	1.90 ± 1.34 (24)	0.96 ± 0.54 (26)	1.08 ± 0.52 (23)
Pausing	1.48 ± 0.95 (9)	2.12 ± 1.78 (26)	1.53 ± 1.57 (5)	1.91 ± 1.95 (19)
Event length changes (μm)				
Growing	1.57	1.51	1.24	1.49
Shrinking	1.63	1.62	1.31	1.38
Total times (%)				
Growing	47	33	48	31
Shrinking	30	30	38	27
Pausing	19	36	12	40
Dynamicity (dimers/s)	18.18	9.95	23.60	15.81

For *STU2* cells in G1, 8 time-lapse sequences lasting a total of 4,274 s were obtained; in preanaphase, 11 time-lapse sequences lasting a total of 3911 s were obtained. For *stu2^{cu}* cells in G1, 14 time-lapse sequences lasting a total of 9123 s were obtained; in preanaphase, 12 time-lapse sequences lasting a total of 5465 s were obtained. Event rates and durations are average values \pm SD. Values in parentheses are the number of events. Event length changes equal mean event rates times mean event durations.

The dynamic properties of cytoplasmic microtubules in *STU2* cells were similar in G1 and preanaphase cells. There was no statistically significant difference in the growth or shrinkage rates of microtubules between G1 and preanaphase cells. Both the catastrophe and rescue frequencies were slightly higher in preanaphase cells.

Stu2p depletion did not have a dramatic effect on the growth or shrinkage rates of cytoplasmic microtubules. The only statistically significant rate difference between *STU2* and *stu2^{cu}* cells was in the shrinkage rates observed in G1 ($p = 0.014$). This latter rate was 1.8-fold lower in *stu2^{cu}* cells (0.85 vs. $1.55 \mu\text{m}/\text{min}$ in *STU2* cells). Similarly, the average duration of growth and shrinkage events in *STU2* and *stu2^{cu}* cells were not significantly different, with the exception again of shrinkage events in G1 cells ($p = 0.011$). The average duration of these latter events was 1.8-fold greater in *stu2^{cu}* cells (1.90 min vs. 1.05 min in *STU2* cells). This increase in duration compensated for the decrease in rate so that average length change of shrinkage events in G1 was nearly identical in *STU2* and *stu2^{cu}* cells (1.63 vs. 1.62 μm , respectively).

In contrast with the above parameters, there was a consistent difference in the transition frequencies of cytoplasmic microtubules in *STU2* and *stu2^{cu}* cells. During G1, the catastrophe frequency was 2-fold lower in *stu2^{cu}* cells (0.0035/s vs. 0.0071/s in *STU2* cells) and the rescue frequency 2.1-fold lower (0.0030/s vs. 0.0063/s in *STU2* cells). In preanaphase *stu2^{cu}* cells, the catastrophe frequency was 1.6-fold lower (0.0054 vs. 0.0085 in *STU2* cells) and the rescue frequency 2.4-fold lower (0.0038 vs. 0.0092 in *STU2* cells). Microtubules in *stu2^{cu}* cells also exhibited a marked increase in the amount of time spent in the paused state. In G1, microtubules in *stu2^{cu}* cells spent 36% of the time pausing compared with

19% for microtubules in *STU2* cells. During preanaphase, microtubules in *stu2^{cu}* cells spent 40% of the time pausing compared with 12% for microtubules in *STU2* cells.

Dynamicity is a measure of the mean rate of tubulin exchange on microtubules and is equivalent to the number of tubulin dimers gained or lost per second (Toso *et al.*, 1993). Differences in dynamicity between microtubules in *STU2* and *stu2^{cu}* cells reflects differences in their growth and shrinkage rates as well as differences in the fraction of time spent growing and shrinking. During G1, the dynamicity of cytoplasmic microtubules in *stu2^{cu}* cells was 10 dimers/s, 1.8-fold lower than the *STU2* rate of 18 dimers/s. In preanaphase cells, the dynamicity of cytoplasmic microtubules in *stu2^{cu}* cells was 16 dimers/s, 1.5-fold lower than the *STU2* rate of 24 dimers/s.

In summary, Stu2p depletion produces microtubules that are significantly less dynamic, with less frequent catastrophes and rescues, and more time spent in pauses. Taken together, these results indicate that Stu2p promotes dynamics of cytoplasmic microtubules in vivo.

Stu2p Depletion Causes a Spindle Orientation Defect

In yeast, cytoplasmic microtubules are required to orient the spindle in a two-step process (Stearns, 1997; Bloom, 2000). Before anaphase, the spindle moves to the bud neck and becomes oriented along the mother-bud axis, a process involving actin cables, Myo2p, Kar9p, Bim1p, and Kip3. At anaphase onset, the spindle traverses the bud neck in a second process involving the dynein heavy chain protein, Dhc1p. These steps are partially redundant; either one is sufficient for cell viability, but loss of both results in lethality.

As cells lacking Stu2p contain fewer and less dynamic cytoplasmic microtubules, we asked whether these changes affect the ability of cytoplasmic microtubules to orient spindles. We grew *stu2^{cu}* cells expressing GFP-Tub1p in copper-containing medium for at least 4 h and obtained random images of spindles in live cells. As a control, *STU2* cells expressing GFP-Tub1p were treated with hydroxyurea to arrest them with preanaphase spindles. We measured the distance of the closest end of the spindle to the mother-bud neck and the angle of the spindle relative to the mother-bud axis (Figure 3B). The position and angle of preanaphase spindles appeared random in *stu2^{cu}* cells. The mean spindle-to-bud neck distance was $2.2 \pm 1.1 \mu\text{m}$ in *stu2^{cu}* cells vs. $1.0 \pm 0.5 \mu\text{m}$ in *STU2* cells ($n = 98, 117$; $p < 0.001$). The mean spindle orientation angle was $53 \pm 25^\circ$ in *stu2^{cu}* cells vs. $22 \pm 19^\circ$ in *STU2* cells ($n = 98, 117$; $p < 0.001$).

The defect observed in *stu2^{cu}* cells is indicative of a block in the early pathway of spindle orientation. Genetic experiments, with the use of two temperature-sensitive alleles of *STU2*, *stu2-10* and *stu2-13*, were consistent with this interpretation. *stu2-10* and *stu2-13* strains were crossed to strains containing either a deletion of *KAR9* (*kar9 Δ*) or *DHC1* (*dhc1 Δ*), and the double mutants were analyzed. Both *stu2-10 kar9 Δ* and *stu2-13 kar9 Δ* double mutants grew well. However, a large fraction of the *stu2-10 dhc1 Δ* and *stu2-13 dhc1 Δ* double mutant spores were inviable (30% and 60%, respectively) and those that were viable grew slowly. Because only cells compromised in both pathways display growth defects, these results are consistent with Stu2p playing a role in the early Kar9p-dependent pathway for spindle orientation.

Kinetochores Microtubules Are Less Dynamic in *Stu2p*-depleted Cells

The haploid *S. cerevisiae* spindle contains 16 kinetochore microtubules originating from each SPB, one for each of the 16 sets of duplicated chromosomes. Each SPB also nucleates ~4 polar microtubules that interdigitate with their counterparts from the opposite pole (Winey *et al.*, 1995). This high density of microtubules makes it impossible to observe the dynamics of individual microtubules in the spindle. Instead, we have used fluorescence redistribution after photobleaching (FRAP) as a measure of spindle microtubule dynamics. In a previous study, Maddox *et al.* (2000) provided evidence that FRAP of yeast preanaphase spindles is a measure of kinetochore microtubule dynamics. Kinetochore microtubule turnover is likely due to the growth and shortening of these microtubules, coupled to oscillations of the chromosomes along the length of the spindle.

Preanaphase spindles labeled with GFP-Tub1p in the *stu2^{cu}* strain were photobleached before and after *Stu2p* depletion. Control cells exhibited fluorescence recovery of $64 \pm 9\%$ of the bleached region after 266 ± 7 s ($n = 4$; Figure 5, A and C) with a half-life of ~60 s, similar to previous experiments with the use of wild-type cells (Maddox *et al.*, 2000). The 36% incomplete recovery in these cells is due to photobleaching of a significant fraction of the cellular tubulin. Interestingly, spindles bleached in cells lacking *Stu2p* recovered fluorescence to only $10 \pm 7\%$ after 234 ± 49 s ($n = 9$; Figure 5, B and C). Because of the low percentage of recovery, a half time for recovery could not be accurately

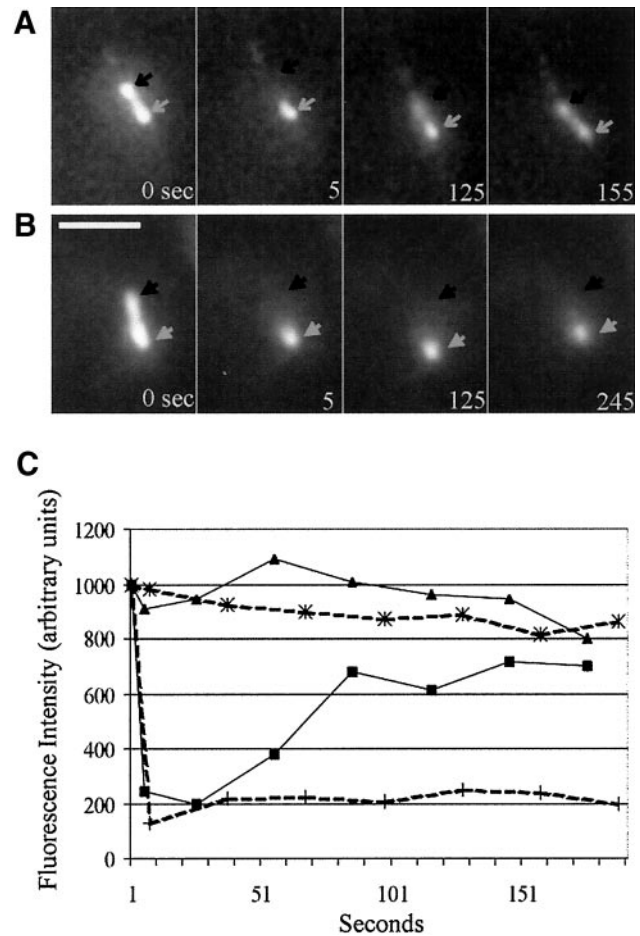


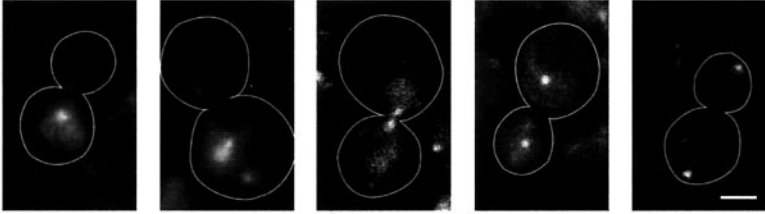
Figure 5. FRAP of *stu2^{cu}* spindles. (A) FRAP of a control cell (CUY1243 grown without copper). (B) FRAP of a cell lacking *Stu2p* (CUY1243 grown with copper). In both A and B, the 0 s time point shows the spindle before laser exposure. Time point 5 s shows the same spindle for each condition after a laser pulse. The cell was followed by 3D time-lapse imaging for a total of 5 min. The control spindle shows fluorescence recovery of the targeted region of the spindle (A, black arrows). However, the bleached region of the *Stu2p*-depleted spindle (B, black arrows) displays attenuated recovery. (C) Quantitation of the fluorescence recovery of a cell lacking *Stu2p* (dotted lines) and a control cell (solid lines). Bleached (squares) and unbleached (triangles) half spindles of a control cell. Bleached (crosses) and unbleached (stars) half spindles of a *Stu2p*-depleted cell.

calculated. These data indicate that spindle microtubule dynamics are substantially attenuated in the absence of *Stu2p*.

Stu2p Depletion Inhibits Metaphase Chromosome Alignment

Kinetochore microtubule dynamics are believed to be essential for chromosome capture and alignment. Because cells lacking *Stu2p* contain less dynamic kinetochore microtubules, we tested whether this decrease in dynamics affects chromosome alignment. In *S. cerevisiae* chromatin arms remain associated until anaphase, but the centromere-proxi-

Figure 6. Centromere localization in *stu2^{cu}* cells. Population counts of Cse4-GFP fluorescence morphologies in control cells (KBY2660.1 grown without copper) and cells lacking Stu2p (KBY2660.1 cells grown with copper for 5 h) determined by acquiring single time-point optical Z-series images. A representative image of each phenotype observed is displayed in the figure, and the percentages of cells in each category are indicated. Cell counts represent the average of four separate experiments. Bar, 2 μ m.



Growth Condition	Focused Cluster	Elongated Cluster	Metaphase		Mid Anaphase (2-4 μ m)	Late Anaphase (>4 μ m)	Total Cells
			< 1 μ m	> 1 μ m			
- copper	1	7	29	21	8	34	241
+ copper	31	21	17	12	18	1	300

mal chromatin is stretched apart into two distinct clusters during metaphase (Goshima and Yanagida, 2000; He *et al.*, 2000; Tanaka *et al.*, 2000; Pearson *et al.*, 2001). This stretched chromatin indicates the presence of poleward pulling forces on the centromeres and provides strong evidence for the existence of tension along the length of the spindle.

We determined the localization of centromeres in *stu2^{cu}* cells expressing Cse4-GFP, a histone H3-like protein that is specifically present at all centromeres (Meluh *et al.*, 1998; Chen *et al.*, 2000). Before depletion of Stu2p, 50% of the large-budded cells exhibited metaphase centromere conformations, characterized by two distinctly separated but clustered foci representing the separated sister centromeres (Figure 6). Forty-two percent exhibited anaphase configurations characterized by two more widely separated (>2 μ m) centromere foci.

After Stu2p depletion most of the large-budded *stu2^{cu}* cells contained preanaphase spindles (see above), but only 48% contained two distinguishable centromere foci (Figure 6). Thirty-one percent contained a single focused cluster, and 21% contained a single elongated cluster, defined as a linear array of \sim 1 μ m with signals of variable intensity along its length. These single cluster morphology classes are distinct from the normal metaphase conformation of two distinguishable foci and indicate either a lack of chromosome attachment or attachment in the absence of force to stretch the centromeres apart. The normal metaphase conformation was observed in only 29% of the *stu2^{cu}* cells. Approximately 18% of *stu2^{cu}* cells had clusters of fluorescence separated by 2–4 μ m, corresponding well to the fraction of partially elongated spindles (15%) observed with the use of GFP-Tub1p fluorescence. Only 1% of the cells had foci separated by >4 μ m. In summary, Stu2p-depletion causes a significant increase in metaphase chromosome misalignment.

Stu2p Localizes to the Spindles, SPBs, and Cytoplasmic Microtubules

We previously described the localization of Stu2-GFP in living cells (Wang and Huffaker, 1997). We reexamined this localization with more sensitive image analysis tools and with the use of a haploid strain in which the endogenous *STU2* gene had been replaced with a single copy of *STU2-GFP* under control of the *STU2* promoter. Consistent with

our previous results, Stu2-GFP fluorescence was concentrated at the spindle pole in all cells at every stage in the cell cycle (Figure 7, A–F). With the more sensitive techniques, Stu2p fluorescence was also seen in a discontinuous manner along the lengths of fibers, presumably cytoplasmic microtubules, in 90% of the unbudded cells. Often the most distal spot was located near the cell cortex and likely represented the tip of the cytoplasmic microtubule, equivalent to the plus end (Figure 7, A and B). In cells with spindles, <50% contained any cytoplasmic staining; this usually occurred as a single dot near the SPB (Figure 7C). Stu2p was located mostly at the poles of short bipolar spindles; in a few cases

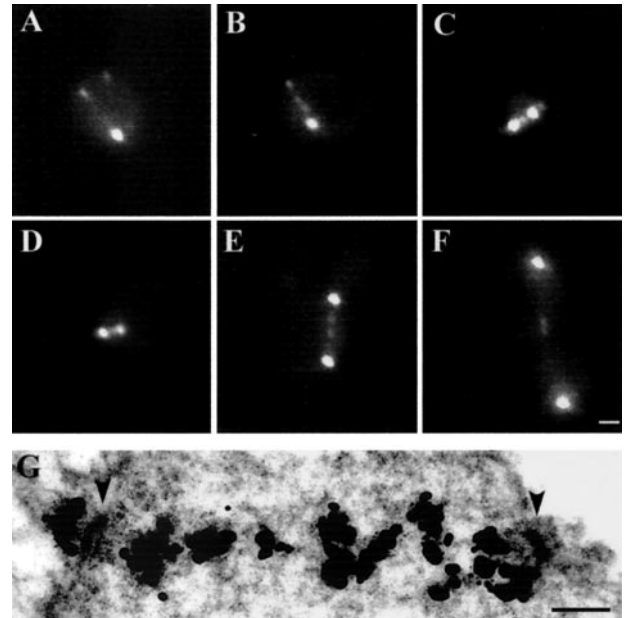


Figure 7. Stu2-GFP localization in vivo. (A–F) Images of GFP fluorescence in living CUY1247 cells expressing Stu2-GFP from the endogenous promoter. These images are either single focal planes (A–D) or compilations created from optical Z-series images (E and F). Bar, 1 μ m. (G) Immunoelectron micrograph of Stu2-GFP with the use of the Nanogold-silver intensification technique (Adams and Kilmartin, 1999). Arrowheads indicate the SPBs. Bar, 0.1 μ m.

an additional single dot was seen between the poles (Figure 7, C and D). As spindles elongated, we occasionally observed Stu2p along their lengths. In these cases, Stu2p localized in a discontinuous manner along the spindle or in one or two dots at the midzone, the location of the plus-ends of overlapping polar microtubules (Figure 7, E and F).

Immunoelectron microscopy was carried out with the use of cells that expressed Stu2-GFP. The GFP antigen was detected on serial sections with the use of the Nanogold-silver intensification method (Adams and Kilmartin, 1999). Stu2p was found near both faces of the SPB indicating that the bright dots observed by Stu2-GFP fluorescence are due to both nuclear and cytoplasmic Stu2p (Figure 7G). In addition, Stu2p was associated with microtubules all along the length of the spindle.

DISCUSSION

The Role of Stu2p in Cytoplasmic Microtubule Function

We have shown that Stu2p plays a prominent role in determining the assembly properties of cytoplasmic microtubules. Depletion of Stu2p led to less dynamic cytoplasmic microtubules in both G1 and preanaphase cells. The decrease in microtubule dynamics is due primarily to twofold decreases in both the catastrophe and rescue frequencies, and a two- to threefold increase in the fraction of time microtubules spend pausing. In G1 cells, the shrinkage rate decreased by nearly twofold as well. On the basis of the phenotype of cells lacking Stu2p, we conclude that Stu2p belongs to the class of microtubule-binding proteins that promote microtubule dynamics.

Although microtubule dynamics decrease in Stu2p-depleted cells, the average cytoplasmic microtubule length determined from static images is not altered. This finding is in agreement with the measured dynamic properties of these microtubules. The average microtubule length change for growth and shrinkage events is very similar in wild-type and Stu2p-depleted cells (Table 2). Thus, Stu2p promotes cytoplasmic microtubule dynamics without affecting overall microtubule length.

Stu2p is localized both to the SPBs and to the distal tips of cytoplasmic microtubules that correspond to the minus and plus ends of microtubules, respectively. There appears to be considerably more Stu2p at the SPB, which might be taken as evidence that Stu2p affects microtubule dynamics primarily at the minus ends of microtubules. However, a recent analysis of fluorescent speckle marks on cytoplasmic microtubules in yeast reveals that there is no detectable assembly or disassembly at minus ends (Maddox *et al.*, 2000). Thus, we favor the interpretation that Stu2p localized at the plus ends of microtubules acts to promote microtubule dynamics.

Stu2p also plays a role in determining cytoplasmic microtubule number. Stu2p-depleted cells contain about half the number of cytoplasmic microtubules as wild-type cells. Cytoplasmic microtubules < 0.5 μm in length cannot be reliably detected by fluorescence microscopy. However, we have no reason to expect that Stu2p-depleted cells possess a significant fraction of very short microtubules, given that the length distributions of the microtubules that we could observe are similar in *STU2* and *stu2^{cu}* cells. Therefore, it seems likely that Stu2p plays a role in controlling microtubule

number that is distinct from its role in controlling microtubule dynamics. One possibility is that Stu2p influences microtubule nucleation. Microtubule assembly is initiated by the γ -tubulin complex that localizes to centrosomes in higher eukaryotes and to SPBs in fungi (Pereira and Schiebel, 1997; Wiese and Zheng, 1999). Localization of the *S. cerevisiae* γ -tubulin complex to the outer plaque or cytoplasmic face of the SPB is mediated by its interaction with the SPB component Spc72p (Knop and Schiebel, 1998). Spc72p also interacts with Stu2p (Chen *et al.*, 1998), raising the intriguing prospect that Stu2p influences γ -tubulin complex activity through Spc72p.

Current models for spindle orientation propose a search-and-capture mechanism whereby dynamic cytoplasmic microtubules find and interact with specific cytoplasmic components. Do the decreases in cytoplasmic microtubule dynamics and number associated with Stu2p-depletion affect their cellular function? Our measurements of spindle orientation demonstrate that they do; in *stu2* mutants, preanaphase spindles are positioned randomly in the mother cell. This phenotype and our genetic data suggest that Stu2p plays a role in the early pathway of spindle orientation. These results likely reflect a greater reliance of the early pathway on the cytoplasmic microtubule dynamics promoted by Stu2p. However, the recent demonstration that Stu2p interacts physically with Kar9p (Miller *et al.*, 2000), a component of the early pathway, suggests that Stu2p may play a more direct role in spindle orientation as well.

The Role of Stu2p in Kinetochores Microtubule Function

The yeast preanaphase spindle contains ~40 microtubules, making it impossible to observe the dynamics of any single spindle microtubule. Instead, we have used FRAP to measure the dynamics of kinetochores microtubules (Maddox *et al.*, 2000). We found that FRAP is substantially reduced in Stu2p-depleted cells. As we did not observe any differences in morphology or fluorescence intensity between preanaphase spindles in wild-type and Stu2p-depleted cells, we do not believe this result is due to a significant decrease in kinetochores microtubule number in the Stu2p-depleted cells. Instead, the lack of FRAP in the absence of Stu2p likely indicates a dramatic decrease in kinetochores microtubule turnover. Extrapolating from studies demonstrating that astral and polar microtubule minus ends do not grow or shorten (Maddox *et al.*, 2000), we conclude that Stu2p plays a key role in promoting plus-end dynamics of kinetochores microtubules.

Dynamic microtubules are thought to be essential for the search-and-capture mechanism proposed for the attachment of microtubules to kinetochores. In addition, dynamic microtubules are likely to be required to generate tension across the spindle. To investigate whether the loss of kinetochores microtubule dynamics affects chromosome alignment, we localized the centromere protein, Cse4-GFP, in Stu2p-depleted cells. Over half of the large-budded Stu2p-depleted cells contain only a single cluster of Cse4p staining, indicating that the sister centromeres are not separated in these cells. Single clusters of Cse4p are rarely seen in wild-type cells and could reflect deficiency in either bipolar attachment or microtubule-mediated tension in the absence of Stu2p. Forty percent of the single clusters in Stu2p-depleted

cells are elongated, a pattern that appears to be intermediate between the single focus and the metaphase arrangement of two foci. Therefore, elongated clusters may represent prometaphase arrangements of centromeres in yeast. Only 30% of the Stu2p-depleted cells contain two foci of Cse4p typical of metaphase. Given the high percentage of Stu2p-depleted cells that show a cell cycle arrest, it seems likely that even some of these cells with two Cse4p foci contain defective spindles that continue to activate the spindle assembly checkpoint. A single unattached kinetochore is sufficient to activate the checkpoint in vertebrates (Rieder *et al.*, 1995) but would be difficult to detect as aberrant Cse4p localization. In summary, our data provide *in vivo* evidence that kinetochore microtubule dynamics are essential for efficient kinetochore attachment and/or spindle tension.

The Role of Stu2p in Polar Microtubule Function

It has recently been reported that a temperature-sensitive allele of *STU2* blocks anaphase B spindle elongation (Severin *et al.*, 2001). Elimination of the spindle checkpoint does allow cells to progress through the cell cycle but does not abrogate the spindle elongation defect, indicating that Stu2p plays a structural role in spindle elongation. Stu2p-depleted cells also fail to elongate spindles. A few Stu2p-depleted cells begin spindle elongation, but these spindles break at ~3–5 μm in length. This breakage could be due to a weak arrangement of polar microtubules or to a defect in elongating these microtubules once anaphase begins. We have not been able to measure the effect of Stu2p depletion on the dynamics of polar microtubules. But given that Stu2p promotes the dynamics of cytoplasmic and kinetochore microtubules, it seems reasonable to propose that Stu2p may promote the dynamics of polar microtubules as well. Consistent with this hypothesis, Stu2p localizes to the midregion of spindles, where the plus-ends of the polar microtubules reside. As polar microtubules must find their counterparts from the opposite pole, decreasing microtubule dynamics could impede this process and lead to the assembly of defective spindles that are unable to elongate. Alternatively, Stu2p may be involved in the switch that allows polar microtubules to lengthen at anaphase B onset. Although Stu2p depletion does not alter the length of cytoplasmic microtubules, it may have a different effect on polar microtubules. The nucleus and the cytoplasm likely contain distinct sets of proteins capable of influencing microtubule dynamics, so the relative contribution of Stu2p to microtubule assembly may differ in these two compartments.

Stu2p and XMAP215

Contrary to the role of XMAP215 that dampens microtubule dynamics in *Xenopus* extracts, Stu2p promotes microtubule dynamics in yeast. These opposite effects may reflect differences in the intrinsic activities of these two proteins, a property that has not yet been determined for Stu2p. However, it seems likely that this discrepancy results, at least in part, from differences in growing yeast cells and *Xenopus* egg extracts. Microtubules in yeast are considerably less dynamic than microtubules in *Xenopus* extracts and animal cells in general (Carminati and Stearns, 1997; Shaw *et al.*, 1997b). This is probably due in part to the fact that tubulin from yeast is inherently less dynamic than tubulin from

animal cells (Davis *et al.*, 1993) and in part to variations in the arrays of proteins that regulate microtubule dynamics in these two systems. Thus, the differences in the roles of Stu2p and XMAP215 may reflect differences in their intrinsic properties or in the environment in which they operate or both.

ACKNOWLEDGMENTS

We thank Arshad Desai and Jennifer Tirnauer for their generous advice. Strains and reagents were kindly provided by Richard Baker, Brendan Cormack, John Kilmartin, Rita Miller and Mark Rose, Zarmik Moqtaderi and Kevin Struhl, and Andrew Murray. For critical comments on the manuscript, we thank Michael Goldberg and Beth Lalonde. This work was supported by grants from the National Institutes of Health (GM40479 to T.C.H., GM32238 to K.B. and GM24364 to E.D.S.)

REFERENCES

- Adames, N.R., and Cooper, J.A. (2000). Microtubule interactions with the cell cortex causing nuclear movements in *Saccharomyces cerevisiae*. *J. Cell Biol.* 149, 863–874.
- Adams, I.R., and Kilmartin, J.V. (1999). Localization of core spindle pole body (SPB) components during SPB duplication in *Saccharomyces cerevisiae*. *J. Cell Biol.* 145, 809–823.
- Bloom, K. (2000). It's a kar9ochore to capture microtubules [news]. *Nat. Cell Biol.* 2, E96–E98.
- Carminati, J.L., and Stearns, T. (1997). Microtubules orient the spindle in yeast through dynein-dependent interactions with the cell cortex. *J. Cell Biol.* 138, 629–642.
- Cassimeris, L. (1999). Accessory protein regulation of microtubule dynamics throughout the cell cycle. *Curr. Opin. Cell Biol.* 11, 134–141.
- Charrasse, S., Schroeder, M., Gauthier-Rouviere, C., Ango, F., Cassimeris, L., Gard, D.L., and Larroque, C. (1998). The TOGp protein is a new human microtubule-associated protein homologous to the *Xenopus* XMAP215. *J. Cell Sci.* 111, 1371–1383.
- Chen, X.P., Yin, H., and Huffaker, T.C. (1998). The yeast spindle pole body component Spc72p interacts with Stu2p and is required for proper microtubule assembly. *J. Cell Biol.* 141, 1169–1179.
- Chen, Y., Baker, R.E., Keith, K.C., Harris, K., Stoler, S., and Fitzgerald-Hayes, M. (2000). The N terminus of the centromere H3-like protein Cse4p performs an essential function distinct from that of the histone fold domain. *Mol. Cell Biol.* 20, 7037–7048.
- Cormack, B.P., Bertram, G., Egerton, M., Gow, N.A., Falkow, S., and Brown, A.J. (1997). Yeast-enhanced green fluorescent protein (yEGFP) a reporter of gene expression in *Candida albicans*. *Microbiology* 143, 303–311.
- Cullen, C.F., Deak, P., Glover, D.M., and Ohkura, H. (1999). Mini spindles: a gene encoding a conserved microtubule-associated protein required for the integrity of the mitotic spindle in *Drosophila*. *J. Cell Biol.* 146, 1005–1018.
- Davis, A., Sage, C.R., Wilson, L., and Farrell, K.W. (1993). Purification and biochemical characterization of tubulin from the budding yeast *Saccharomyces cerevisiae*. *Biochemistry* 32, 8823–8835.
- Desai, A., and Mitchison, T.J. (1997). Microtubule polymerization dynamics. *Annu. Rev. Cell Dev. Biol.* 13, 83–117.
- Goshima, G., and Yanagida, M. (2000). Establishing biorientation occurs with precocious separation of the sister kinetochores, but not the arms, in the early spindle of budding yeast. *Cell* 100, 619–633.
- Haase, S.B., and Lew, D.J. (1997). Flow cytometric analysis of DNA content in budding yeast. *Methods Enzymol.* 283, 322–332.

- He, X., Asthana, S., and Sorger, P.K. (2000). Transient sister chromatid separation and elastic deformation of chromosomes during mitosis in budding yeast. *Cell* 101, 763–775.
- Kilmartin, J.V., Wright, B., and Milstein, C. (1982). Rat monoclonal antitubulin antibodies derived by using a new nonsecreting rat cell line. *J. Cell Biol.* 93, 576–582.
- Knop, M., and Schiebel, E. (1998). Receptors determine the cellular localization of a gamma-tubulin complex and thereby the site of microtubule formation. *EMBO J.* 17, 3952–3967.
- Maddox, P.S., Bloom, K.S., and Salmon, E.D. (2000). The polarity and dynamics of microtubule assembly in the budding yeast *Saccharomyces cerevisiae*. *Nat. Cell Biol.* 2, 36–41.
- Matthews, L.R., Carter, P., Thierry-Mieg, D., and Kemphues, K. (1998). ZYG-9, a *Caenorhabditis elegans* protein required for microtubule organization and function, is a component of meiotic and mitotic spindle poles. *J. Cell Biol.* 141, 1159–1168.
- Meluh, P.B., Yang, P., Glowczewski, L., Koshland, D., and Smith, M.M. (1998). Cse4p is a component of the core centromere of *Saccharomyces cerevisiae*. *Cell* 94, 607–613.
- Miller, R.K., Cheng, S.C., and Rose, M.D. (2000). Bim1p/Yeb1p mediates the Kar9p-dependent cortical attachment of cytoplasmic microtubules. *Mol. Biol. Cell* 11, 2949–2959.
- Moqtaderi, Z., Bai, Y., Poon, D., Weil, P.A., and Struhl, K. (1996). TBP-associated factors are not generally required for transcriptional activation in yeast. *Nature* 383, 188–191.
- Muhlrads, D., Hunter, R., and Parker, R. (1992). A rapid method for localized mutagenesis of yeast genes. *Yeast* 8, 79–82.
- Nabeshima, K., Kurooka, H., Takeuchi, M., Kinoshita, K., Nakaseko, Y., and Yanagida, M. (1995). p93dis1, which is required for sister chromatid separation, is a novel microtubule and spindle pole body-associating protein phosphorylated at the Cdc2 target sites. *Genes Dev.* 9, 1572–1585.
- Pasqualone, D., and Huffaker, T.C. (1994). *STU1*, a suppressor of a β -tubulin mutation, encodes a novel and essential component of the yeast mitotic spindle. *J. Cell Biol.* 127, 1973–1984.
- Pearson, C.G., Maddox, P.S., Salmon, E.D., and Bloom, K. (2001). Budding yeast chromosome structure and dynamics during mitosis. *J. Cell Biol.* 152, 1255–1266.
- Pereira, G., and Schiebel, E. (1997). Centrosome-microtubule nucleation. *J. Cell Sci.* 110, 295–300.
- Rieder, C.L., Cole, R.W., Khodjakov, A., and Sluder, G. (1995). The checkpoint delaying anaphase in response to chromosome monoorientation is mediated by an inhibitory signal produced by unattached kinetochores. *J. Cell Biol.* 130, 941–948.
- Severin, F., Habermann, B., Huffaker, T., and Hyman, T. (2001). Stu2 promotes mitotic spindle elongation in anaphase. *J. Cell Biol.* 153, 435–442.
- Shaw, S.L., Yeh, E., Bloom, K., and Salmon, E.D. (1997a). Imaging green fluorescent protein fusion proteins in *Saccharomyces cerevisiae*. *Curr. Biol.* 7, 701–704.
- Shaw, S.L., Yeh, E., Maddox, P., Salmon, E.D., and Bloom, K. (1997b). Astral microtubule dynamics in yeast: a microtubule-based searching mechanism for spindle orientation and nuclear migration into the bud. *J. Cell Biol.* 139, 985–994.
- Sherman, F. (1991). Getting started with yeast. *Methods Enzymol.* 194, 3–21.
- Sikorski, R.S., and Hieter, P. (1989). A system of shuttle vectors and yeast host strains designed for efficient manipulation of DNA in *Saccharomyces cerevisiae*. *Genetics* 122, 19–27.
- Sorger, P.K., Severin, F.F., and Hyman, A.A. (1994). Factors required for the binding of reassembled yeast kinetochores to microtubules in vitro. *J. Cell Biol.* 127, 995–1008.
- Stearns, T. (1997). Motoring to the finish: kinesin and dynein work together to orient the yeast mitotic spindle [comment]. *J. Cell Biol.* 138, 957–960.
- Straight, A.F., Marshall, W.F., Sedat, J.W., and Murray, A.W. (1997). Mitosis in living budding yeast: anaphase A but no metaphase plate. *Science* 277, 574–578.
- Sullivan, D.S., and Huffaker, T.C. (1992). Astral microtubules are not required for anaphase B in *Saccharomyces cerevisiae*. *J. Cell Biol.* 119, 379–388.
- Tanaka, T., Fuchs, J., Loidl, J., and Nasmyth, K. (2000). Cohesin ensures bipolar attachment of microtubules to sister centromeres and resists their precocious separation. *Nat. Cell Biol.* 2, 492–499.
- Tirnauer, J.S., O'Toole, E., Berrueta, L., Bierer, B.E., and Pellman, D. (1999). Yeast Bim1p promotes the G1-specific dynamics of microtubules. *J. Cell Biol.* 145, 993–1007.
- Toso, R.J., Jordan, M.A., Farrell, K.W., Matsumoto, B., and Wilson, L. (1993). Kinetic stabilization of microtubule dynamic instability in vitro by vinblastine. *Biochem.* 32, 1285–1293.
- Tournebize, R., Popov, A., Kinoshita, K., Ashford, A.J., Rybina, S., Pozniakovskiy, A., Mayer, T.U., Walczak, C.E., Karsenti, E., and Hyman, A.A. (2000). Control of microtubule dynamics by the antagonistic activities of XMAP215 and XKCM1 in *Xenopus* egg extracts. *Nat. Cell Biol.* 2, 13–19.
- Vasquez, R.J., Gard, D.L., and Cassimeris, L. (1994). XMAP from *Xenopus* eggs promotes rapid plus end assembly of microtubules and rapid microtubule polymer turnover. *J. Cell Biol.* 127, 985–993.
- Wang, P.J., and Huffaker, T.C. (1997). Stu2p: a microtubule-binding protein that is an essential component of the yeast spindle pole body. *J. Cell Biol.* 139, 1271–1280.
- Wiese, C., and Zheng, Y. (1999). Gamma-tubulin complexes and their interaction with microtubule-organizing centers. *Curr. Opin. Struct. Biol.* 9, 250–259.
- Winey, M., Mamay, C.L., O'Toole, E.T., Mastrorarde, D.N., Giddings, Jr., T.H., McDonald, K.L., and McIntosh, J.R. (1995). Three-dimensional ultrastructural analysis of the *Saccharomyces cerevisiae* mitotic spindle. *J. Cell Biol.* 129, 1601–1615.